Andrographolide induces degradation of mutant p53 via activation of Hsp70

HIROFUMI SATO[1], MASATSUGU HIRAKI[1], TAKUSHI NAMBA[2], NORIYUKI EGAWA[1], KOICHI BABA[1], TOMOKAZU TANAKA[1] and HIROKAZU NOSHIRO[1]

[1]Department of Surgery, Faculty of Medicine, Saga University, Saga, Saga 849-8501; [2]Science Research Center, Kochi University, Nankoku-shi, Kochi 783-8505, Japan

Received December 12, 2017; Accepted March 30, 2018

DOI: 10.3892/ijo.2018.4416

Abstract. The tumor suppressor gene p53 encodes a transcription factor that regulates various cellular functions, including DNA repair, apoptosis and cell cycle progression. Approximately half of all human cancers carry mutations in p53 that lead to loss of tumor suppressor function or gain of functions that promote the cancer phenotype. Thus, targeting mutant p53 as an anticancer therapy has attracted considerable attention. In the current study, a small-molecule screen identified andrographlide (ANDRO) as a mutant p53 suppressor. The effects of ANDRO, a small molecule isolated from the Chinese herb *Andrographis paniculata*, on tumor cells carrying wild-type or mutant p53 were examined. ANDRO suppressed expression of mutant p53, induced expression of the cyclin-dependent kinase inhibitor p21 and pro-apoptotic proteins genes, and inhibited the growth of cancer cells harboring mutant p53. ANDRO also induced expression of the heat-shock protein (Hsp70) and increased binding between Hsp70 and mutant p53 protein, thus promoting proteasomal degradation of p53. These results provide novel insights into the mechanisms regulating the function of mutant p53 and suggest that activation of Hsp70 may be a new strategy for the treatment of cancers harboring mutant p53.

Introduction

The transcription factor p53 is activated in response to various stresses, including DNA damage, nutrient deprivation, oncogene activation and hypoxia (1). p53 is a well-established tumor suppressor and 'guardian of the genome' that induces cell cycle arrest and apoptosis by activating downstream target genes (2). However, p53 is mutated in around half of all human cancers (3), leading to loss of its tumor suppressor activity and, in certain cases, gain-of-function activities (4) that promote cell proliferation, tumor development, and drug resistance (5,6). Thus, mutant p53 has become an important target for the development of anticancer treatments. A number of small molecule targeted to mutant p53 have been described, most of which promote the proteasomal or autophagic degradation of mutant p53 or restoration of wild-type p53 function. The current study identified andrographolide (ANDRO), a labdane diterpenoid isolated from the Chinese herb *Andrographis paniculata*, as a mutant p53 suppressor from a small-molecule screen, and investigated the effects of ANDRO on human cancer cell lines harboring mutant or wild-type p53. ANDRO suppressed the activity of mutant p53 and the growth of cancer cells via induction of the heat shock protein (Hsp) 70, resulting in enhanced proteasomal degradation of mutant p53. ANDRO also effectively reduced the growth of mutant p53 tumors in a mouse xenograft model.

Correspondence to: Dr Masatsugu Hiraki, Department of Surgery, Faculty of Medicine, Saga University, 5-1-1 Nabeshima, Saga, Saga 849-8501, Japan
E-mail: masatsuguhiraki@hotmail.com

Key words: mutant p53, andrographolide, heat shock protein 70

Materials and methods

Cell lines and culture conditions. All cell lines were obtained from RIKEN BioResource Center (Tsukuba, Japan). PANC-1 (human pancreatic cancer) and HCT116 (human colorectal cancer) were maintained in Dulbecco's modified Eagle's medium (DMEM; Sigma-Aldrich; Merck KGaA, Darmstadt, Germany). HuCCT1 (human bile duct cancer) and MKN45 (human gastric cancer) were maintained in RPMI-1640 medium (Sigma-Aldrich; Merck KGaA). DMEM and RPMI-1640 media were supplemented with 10% fetal bovine serum (Sigma-Aldrich; Merck KGaA) and 100 μg/ml kanamycin (Meiji Seika Pharma Co., Ltd., Tokyo, Japan). The cell lines were maintained at 37˚C in a humidified atmosphere containing 20% O_2 and 5% CO_2.

Chemicals. ANDRO, acacetin, berberine, honokiol, pentamidine, 3-(5'-hydroxymethyl-2'-furyl)-1-benzyl indazole (YC-1), and 2-mercaptoethanol (2-ME) were purchased from Sigma-Aldrich (Merck KGaA). Noscapine and irinotecan (CPT-11) were obtained from Tokyo Chemical Industry Co., Ltd. (Tokyo, Japan). The compounds were dissolved in dimethyl sulfoxide (DMSO) and stored at -20˚C prior to use. For experiments, the compounds were diluted in medium to the appropriate doses immediately prior to use. These compounds

were used as indicated or at the following concentrations: ANDRO, 100 μM; acacetin, 100 μM; berbeline, 50 μM; honokiol, 50 μM; noscapine, 100 μM; pentamigine, 200 μM; YC-1, 100 μM; 2-ME, 30 μM.

Immunoblotting. Cells were plated in 60 mm dishes and allowed to grow to 60-70% confluence. The cells were then treated with the appropriate reagents for 18 h and lysed in lysis buffer consisting of 150 mM NaCl, 50 mM Tris-HCl (pH 7.6), protease inhibitor cocktail mix (Roche Diagnostic GmbH, Mannheim, Germany) and phenylmethylsulfonyl fluoride. Proteins (20-37.5 μg/well) were separated by SDS-polyacrylamide gel electrophoresis on 10% gels and electroblotted onto Immobilon membranes (Bio-Rad Laboratories, Inc., Hercules, CA, USA). Membranes were blocked with 5% non-fat milk in 150 mM NaCl, 25 mM Tris pH 7.5 and 0.1% Tween-20 (TBS-T) and probed overnight at 4˚C with primary antibodies diluted 1:500-1:1,000 in the same buffer. Membranes were washed with TBS-T twice for 5 min each and then incubated with secondary antibody (1:1,000 dilution; goat anti-rabbit and goat anti-mouse IgG-horseradish peroxidase; cat nos. sc-2004 and sc-2005; Santa Cruz Biotechnology, Inc., Dallas, TX, USA) for 30 min at room temperature. The blots were developed with enhanced chemiluminescence reagents (Amersham ECL Prime; GE Healthcare, Chicago, IL, USA) and analyzed with a Fujifilm LAS-3000 imaging system (Fujifilm Corporation, Tokyo, Japan). The primary antibodies were specific for: p53 (1:1,000 dilution; clone DO-1; cat no. sc-126), p21 (1:500 dilution; clone C-19; cat. no. sc-397), E3 ubiquitin-protein ligase Mdm2 (1:1,000 dilution; MDM2; clone SMP14; cat. no. sc-965), E3 ubiquitin-protein ligase CHIP (1:500 dilution; CHIP; clone I-16; cat. no. sc-33264) signal transducer and activator of transcription-3 (STAT-3; 1:1,000 dilution; clone C-20; cat. no. sc-482) and Hsp40 (1:1,000 dilution; clone C-20; cat. no. sc1800), all from Santa Cruz Biotechnology, Inc.; Bcl-2-binding component 3 (PUMA; 1:1,000 dilution; cat. no. 7467), caspase-3 (1:1,000 dilution; cat. no. 9662) and Hsp70 (1:1,000 dilution; cat. no. 4873), all Cell Signaling Technology, Inc. (Danvers, MA, USA); phorbol-12-myristate-13-acetate-induced protein 1 (NOXA; 1:1,000 dilution; cat. no. 114C307; Calbiochem; Merck KGaA); Hsp90 (1:1,000 dilution; cat. no. AC88; Enzo Life Sciences, Inc., Farmingdale, NY, USA); cyclin D1 (1:1,000 dilution; cat. no. ab134175; Abcam, Cambridge, UK) and β-actin (1:1,000 dilution; cat. no. A2228; Sigma-Aldrich; Merck KGaA).

Total RNA extraction and reverse transcription-quantitative polymerase chain reaction (RT-qPCR) analysis. Total RNA was extracted using a Qiagen RNA extraction kit, converted to cDNA (37˚C for 15 min for RT, 98˚C for 5 min to terminate the reaction and 12˚C hold) using an iScript cDNA Synthesis kit (Bio-Rad Laboratories, Inc.), and analyzed by qPCR. The gene-specific primer sequences were: p53 forward, 5'-GCC CAACAACACCAGCTCCT-3 and reverse, 5'-CCTGGGCATC CTTGAGTTCC-3'; p21 forward, 5'-GGCGGCAGACCAGCA TGACAGATT-3' and reverse, 5'-GCAGGGGGCGGCCAGGG TAT-3'; PUMA forward, 5'-GACCTCAACGCACAGTAC GAG-3' and reverse, 5'-AGGAGTCCCATGATGAGAT TGT-3'; NOXA forward, 5'-ATTACCGCTGGCCTACTGTG-3' and reverse, 5'-GTGCTGAGTTGGCACTGAAA-3'; heat shock transcription factor 1 forward, 5'-GCCTTCCTGACCAA GCTGT-3' and reverse, 5'-AAGTACTTGGGCAGCACCTC-3'; Hsp40 forward, 5'-GGCTTCACCAACGTGAACTT-3' and reverse, 5'-CGCTTGTGGGAGATTTTCAT-3'; Hsp70 forward, 5'-CAAGATCACCATCACCAACG-3' and reverse, 5'-TCG TCCTCCGCTTTGTACTT-3'; and Hsp90 forward, 5'-GCA GAAATTGCCCAACTCAT-3' and reverse, 5'-AAGGGT CTGTCAGGCTCTCA-3'. qPCR was performed using a CFX Connect™ Real-Time PCR Detection System with PrimePCR™ SYBR® Green Assay reagents (both from Bio-Rad Laboratories, Inc.) according to the manufacturer's instructions. After performing a denaturation step at 95˚C for 3 min, PCR amplification was conducted with 45 cycles of 15 sec of denaturation at 95˚C, 5 sec of annealing at 60˚C and 10 sec of extension at 72˚C. Expression of the gene of interest was normalized to β-actin forward, ACTCTTCCAGCCTTCCTTCC and reverse, GACAGCACTGTGTTGGCGTA, mRNA levels by $2^{-\Delta\Delta Cq}$ method (7). All experiments were performed in triplicate.

Cell viability assay. Cell viability was determined using the Sulforhodamine B-based *In Vitro* Toxicology Assay kit (Sigma-Aldrich; Merck KGaA). Cells were seeded in 6-well plates and allowed to reach 60-70% confluency. Cells were then treated with ANDRO and incubated for a further 24 h. Cell staining and quantification of viability were performed according to the manufacturer's instructions. All experiments were performed in duplicate.

Immunoprecipitation. HuCCT1 and PANC-1 cells were seeded into 150 mm dishes. After 24 h, the cells were treated with ANDRO at 100 μM and incubated for 18 h. Cells were then lysed in lysis buffer as described above. The samples were centrifuged at 16,000 x g for 15 min at 4˚C, and the clarified cell lysates were removed and incubated overnight at 4˚C with 15 μl Protein G plus/Protein A-agarose (cat. no. sc-2003) and 1 μg anti-p53 antibody (clone DO-1; cat no. sc-126) (both from Santa Cruz Biotechnology, Inc.). The beads were then washed three times with lysis buffer. Aliquots of cell lysates (input) or immunoprecipitates were resolved by SDS-PAGE on 10% gels, transferred to nitrocellulose membranes, and probed with specific primary antibodies as described above.

Flow cytometry. Cell cycle analysis was performed by flow cytometry after staining of DNA with propidium iodide (PI). Cells were treated with DMSO or ANDRO at the indicated concentrations for 18 h, harvested by trypsinization, washed with PBS, and fixed in 70% ethanol overnight at 4˚C. The cells were centrifuged, washed twice with PBS, resuspended in 300 μl PBS containing 200 μg/ml of RNase (Wako Pure Chemical Industries, Ltd., Osaka, Japan), and incubated for 30 min at 37˚C. PI (50 μg/ml) was then added and the cells were incubated in the dark for 30 min at 4˚C. Finally, the cells were analyzed using a FACSVerse flow cytometer (BD Biosciences, San Jose, CA, USA) and FlowJo 10.2 software (FlowJo LLC, Ashland, OR, USA).

RNA interference. Small interfering RNAs (siRNAs) were obtained from Santa Cruz Biotechnology, Inc. (siControl, cat. no. sc-37007; siHsp70, cat. no. sc-29352) and transfected into cells using Lipofectamine RNAiMax (Invitrogen; Thermo

Fisher Scientific, Inc.), according to the manufacturer's protocol.

Animal experiments. An animal experimental protocol was reviewed and approved by the Animal Care Committee of Saga University (Saga, Japan; permission no. 27-039-0). A total of 60 female BALB/c mice (4-6 week-old) were purchased from Kyudo Co., Ltd. (Saga, Japan). The animals were maintained in an animal facility in a 12/12 h light/dark cycle in a temperature (20˚C) and humidity-controlled environment. Food and water were freely available. HuCCT1 ($5x10^6$) and MKN45 ($7x10^6$) cells were injected subcutaneously into the flanks of nude mice (n=6/group). Tumor size was monitored using a vernier caliper and the volume was calculated from the length (L) and width (W) using the formula: volume = L x W^2 x $\pi/6$. Treatment was initiated when the tumor volume reached 50 mm^3. The mice were randomly divided into three groups as follows: i) Untreated control (DMSO in PBS); ii) ANDRO 10 mg/kg; and iii) CPT-11 10 mg/kg. All treatments were administered three times per week by intraperitoneal (i.p.) injection. Body weights were also measured three times per week. After 11 days of treatment, the mice were euthanized. The average weight of the mouse at the time of purchase and sacrifice was 18.02±0.47 and 17.69±0.56 g, respectively.

Statistical analysis. Data are expressed as the mean ± standard deviation, and analyses were performed using JMP Pro 12 software (SAS Institute, Inc., Cary, NC, USA). Differences between mean values were evaluated using two-way analysis of variance followed by Tukey's test. $P<0.05$ was considered to indicate a statistically significant difference.

Results

Identification of andrographolide as a mutant p53 suppressor and inducer of p53 target genes. The pancreatic cancer cell line PANC-1, which harbors mutant p53 R273H, was incubated for 18 h with various small molecules to investigate their effects on the expression of p53. The compounds were tested in pilot experiments and the concentrations used were equivalent to the 50% inhibitory concentrations (i.e., induced the death of ~50% of PANC-1 cells in 18 h). Among the compounds tested, only ANDRO reduced the expression of mutant p53 protein (Fig. 1A). The structure of ANDRO is presented in Fig 1B. To examine the expression level of p53 in with different p53 mutation statuses, HuCCT1 (bile duct carcinoma; mutant p53 R175H), HCT116 (colon cancer; wild-type p53), and MKN45 (gastric cancer; wild-type p53) cells were also used. Following treatment of the cells with ANDRO for 18 h, HuCCT1 cells also showed reduced mutant p53 protein levels, whereas expression of wild-type p53 in HCT116 and MKN45 cells was increased (Fig. 1C). The expression of the p53-regulated proteins; p21, which is an inhibitor of cyclin-dependent kinase activity and regulates cell cycle progression, and NOXA, which is pro-apoptotic protein, were also examined. Notably, ANDRO treatment also increased the level of these proteins in cells carrying mutant or wild-type p53 (Fig. 1C). The protein level of mutant p53 was semi-quantified by measuring relative band intensity. The results demonstrated that the expression of mutant p53 protein was decreased by ANDRO in a concentration-dependent manner (Fig. 1D). Finally, mRNA levels of p21, PUMA and NOXA were also increased by ANDRO in a time-dependent manner in the mutant p53-expressing cells HuCCT1 and PANC-1. However, the mRNA level of mutant p53 showed no response to ANDRO (Fig. 1E).

Anticancer effects of ANDRO. To determine whether ANDRO affects cell cycle progression and/or apoptosis, the DNA profiles of PI-stained cells were analyzed by flow cytometry or the expression of cleaved caspase-3, a marker of apoptosis, was determined by immunoblotting (Fig. 2A and B). In the flow cytometric assay, treatment with ANDRO for 24 h induced arrest of HuCCT1 cells in the G1 phase (Fig. 2A). In addition, ANDRO enhanced the expression of cleaved caspase-3 (17 kDa) and decreased the expression of caspase-3 (35 kDa) in HuCCT1 and PANC-1 cells in a dose-dependent manner (Fig. 2B). To verify the anticancer effect of ANDRO, cell viability was analyzed with a Sulforhodamine B assay. The effects of ANDRO were compared with that of the chemotherapeutic drug CPT-11 (irinotecan), which induces apoptosis in a wild-type p53-dependent manner. As presented in Fig. 3, CPT-11 effectively reduced the viability of cell lines harboring wild-type p53, however, it had only a limited effect on cell lines harboring mutant p53. By contrast, ANDRO was more cytotoxic towards cells expressing mutant p53 than those expressing wild-type p53 (Fig. 3).

ANDRO promotes degradation of mutant p53 via induction of Hsp70. To understand how ANDRO reduces the expression of mutant p53, it was hypothesized that ANDRO may destabilize and/or promote the degradation of the mutant protein. The heat-shock proteins are known to directly bind to p53 and regulate its conformation and stability by functioning as chaperones or co-chaperones (8). Therefore, whether ANDRO affected the expression of these heat-shock proteins was examined. Indeed, HuCCT1 and PANC-1 cells treated with ANDRO exhibited increased expression of Hsp40 and Hsp70 mRNA levels (Fig. 4A), and all cell lines, regardless of their p53 status, exhibited increased levels of Hsp40 and Hsp70 protein following ANDRO treatment (Fig. 4B). To determine whether ANDRO increased the binding of Hsp40, Hsp70, or Hsp90 to mutant p53, p53 was immunoprecipitated from control and ANDRO-treated cells and the presence of the heat-shock proteins were probed for by immunoblotting. More Hsp70 was bound to mutant p53 in ANDRO-treated than vehicle-treated HuCCT1 and PANC-1 cells (Fig. 5A), suggesting that Hsp70 may be involved in reducing mutant p53 levels. Consistent with this, siRNA-mediated knockdown of Hsp70 reduced the ANDRO-induced suppression of mutant p53 levels and concomitantly increased the expression of p21 in PANC-1 cells (Fig. 5B).

ANDRO induces proteasomal degradation of mutant p53. As ANDRO promotes the association of mutant p53 with Hsp70, it was subsequently determined whether the enhanced association influenced the stability/degradation of p53. For this, cells were incubated with MG132 (1 μM for 18 h), an inhibitor of proteasomal degradation. Notably, cells incubated with MG132 and ANDRO exhibited higher mutant p53 levels than

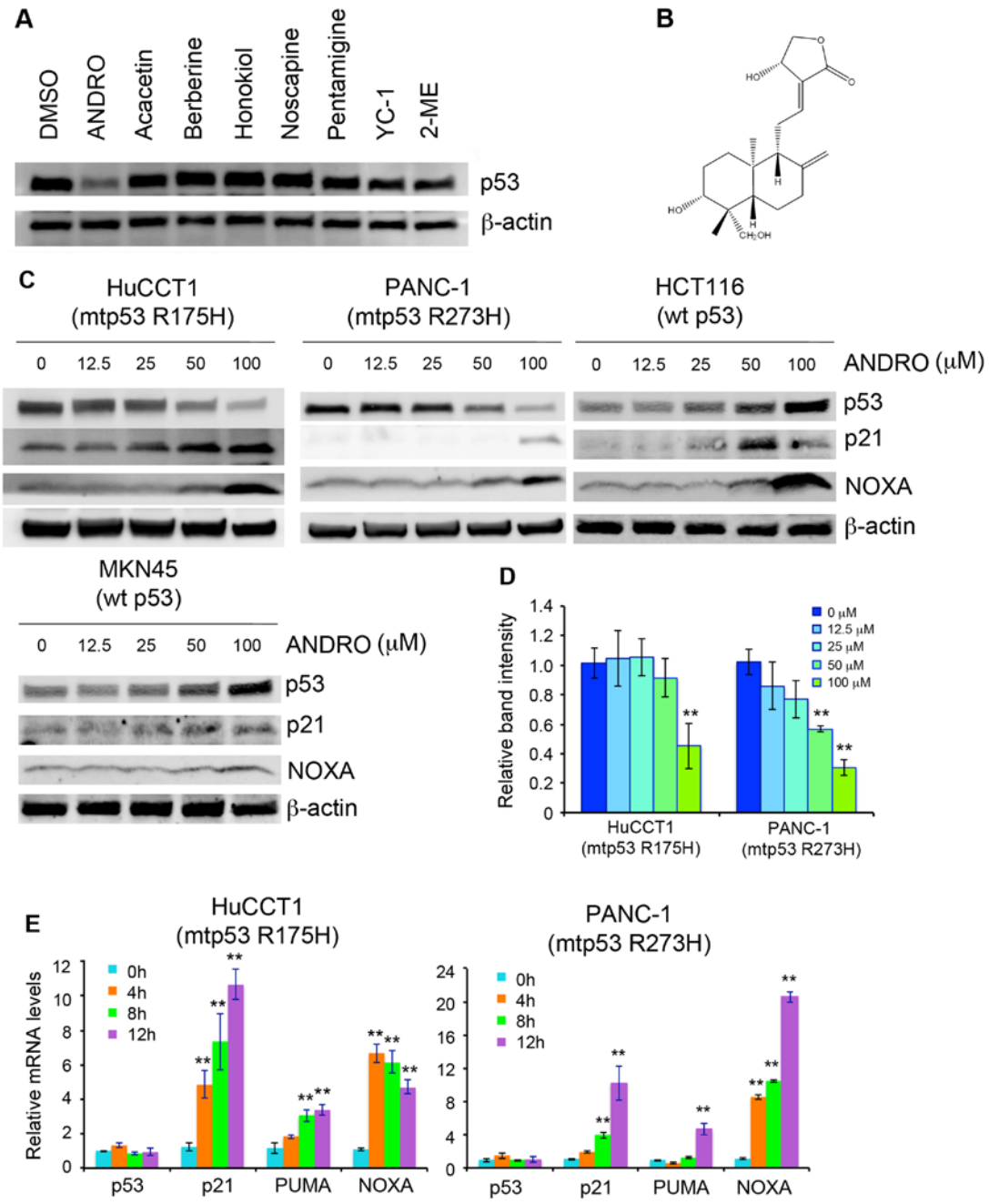

Figure 1. Identification of ANDRO as a suppressor of mutant p53 and inducer of p53 target gene expression. (A) Expression of mutant p53 in PANC-1 cells treated with various small molecules. (B) Chemical structure of ANDRO. (C) Immunoblot analysis of p53 target gene expression in cells treated with ANDRO for 18 h. (D) The intensity of p53 band in three independent experiments was determined by densitometric scanning using ImageJ software and expressed relative to the control. (E) Reverse transcription-quantitative polymerase chain reaction analysis of p53, p21, PUMA, and NOXA mRNA levels after ANDRO treatment. Values are presented as the mean ± standard deviation of three independent experiments performed in triplicate. **P<0.01 vs. 0 h. DMSO, dimethyl sulfoxide; ANDRO, andrographolide; YC-1, 3-(5'-hydroxymethyl-2'-furyl)-1-benzyl indazole; 2-ME, 2-mercaptoethanol; mtp53, mutant p53; wt p53, wild-type p53; NOXA, phorbol-12-myristate-13-acetate-induced protein 1.

those treated with ANDRO, indicating that ANDRO reduced p53 levels by promoting its proteasomal degradation (Fig. 6A). MDM2 and CHIP are ubiquitin ligases known to target mutant p53 for proteasomal degradation (9). However, neither MDM2 nor CHIP was induced by treatment of cells with ANDRO; in fact, MDM2 expression was marginally decreased (Fig. 6B), suggesting that other ubiquitin ligases may be responsible for the enhanced p53 degradation.

Notably, a previous study reported that ANDRO can induce p21 and apoptosis-associated genes via inactivation of STAT-3 (10). Indeed, the expression of STAT-3 and the cell cycle regulatory protein cyclin D1 were decreased by ANDRO treatment of mutant p53-expressing cells in a dose-dependent manner (Fig. 6C), suggesting that ANDRO may induce cell cycle arrest and apoptosis of mutant p53-expressing cells via STAT-3.

Antitumor effect of ANDRO in a mouse xenograft model. It was verified that the anticancer effects of ANDRO were also observed *in vivo* using a mouse xenograft model. HuCCT1

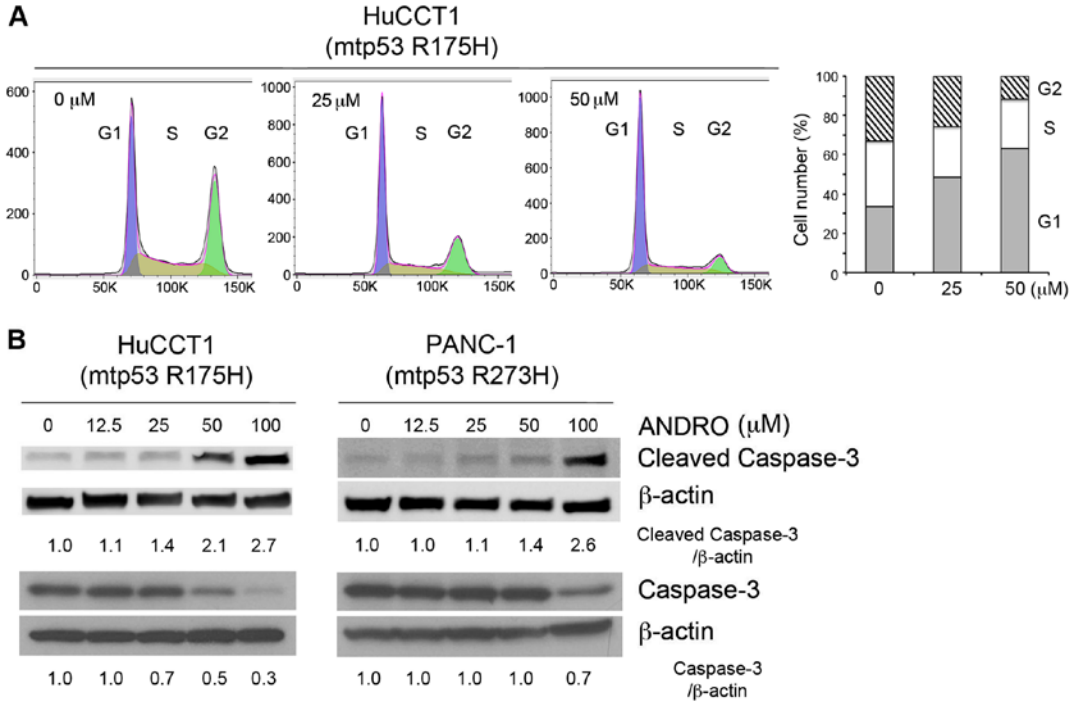

Figure 2. Anticancer effect of ANDRO on cancer cells harboring mutant p53. (A) Flow cytometric analysis of HuCCT1 cell cycle progression after treatment with 0, 25 or 50 μM ANDRO for 24 h. (B) Cleaved caspase-3 and caspase-3 protein levels in cells treated with ANDRO for 18 h. Quantitative analysis was performed on each western blotting by densitometric scanning using ImageJ software. mtp53, mutant p53; ANDRO, andrographolide.

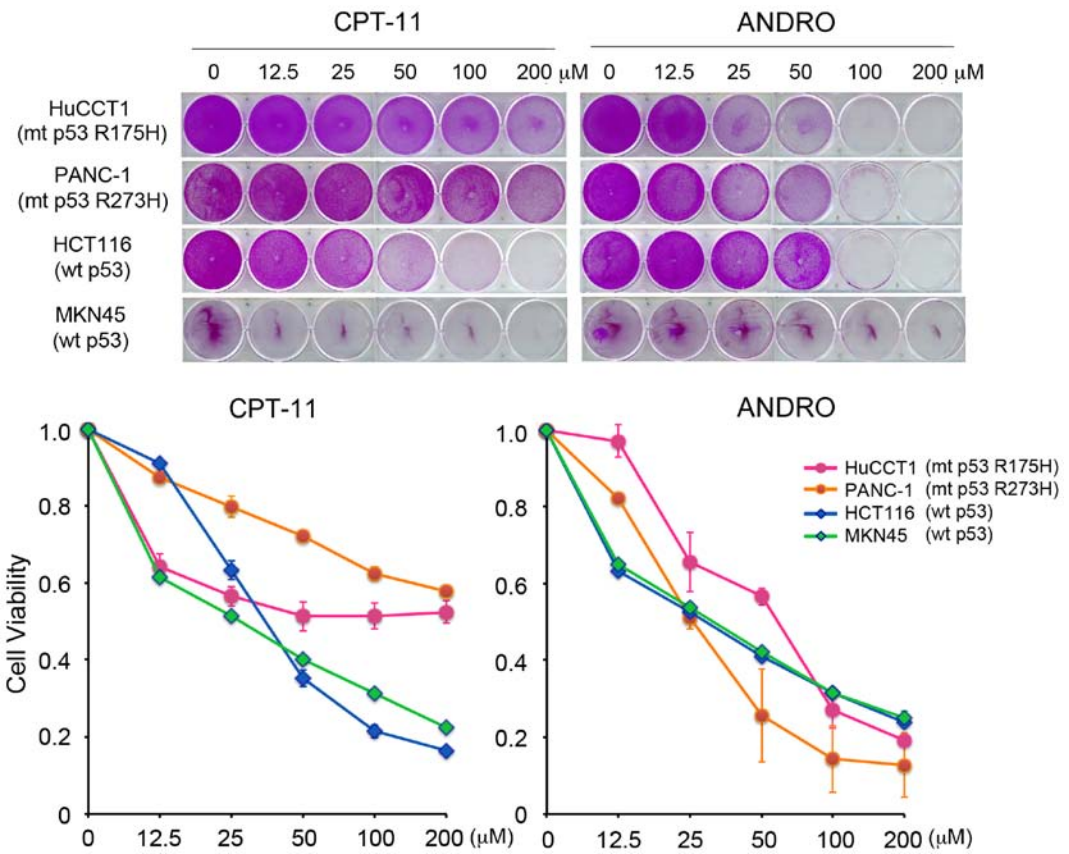

Figure 3. Sulforhodamine B staining of cancer cells treated with various doses of ANDRO and CPT-11 for 48 h. CPT-1, irinotecan; ANDRO, andrographolide; mtp53, mutant p53; wt p53, wild-type p53.

cells (mutant p53 R175H) and MKN45 cells (wild-type p53) were injected subcutaneously into the flanks of nude mice. When the tumors reached 50 mm^3 the mice were treated with vehicle (DMSO in PBS), ANDRO (10 mg/kg), or CPT-11

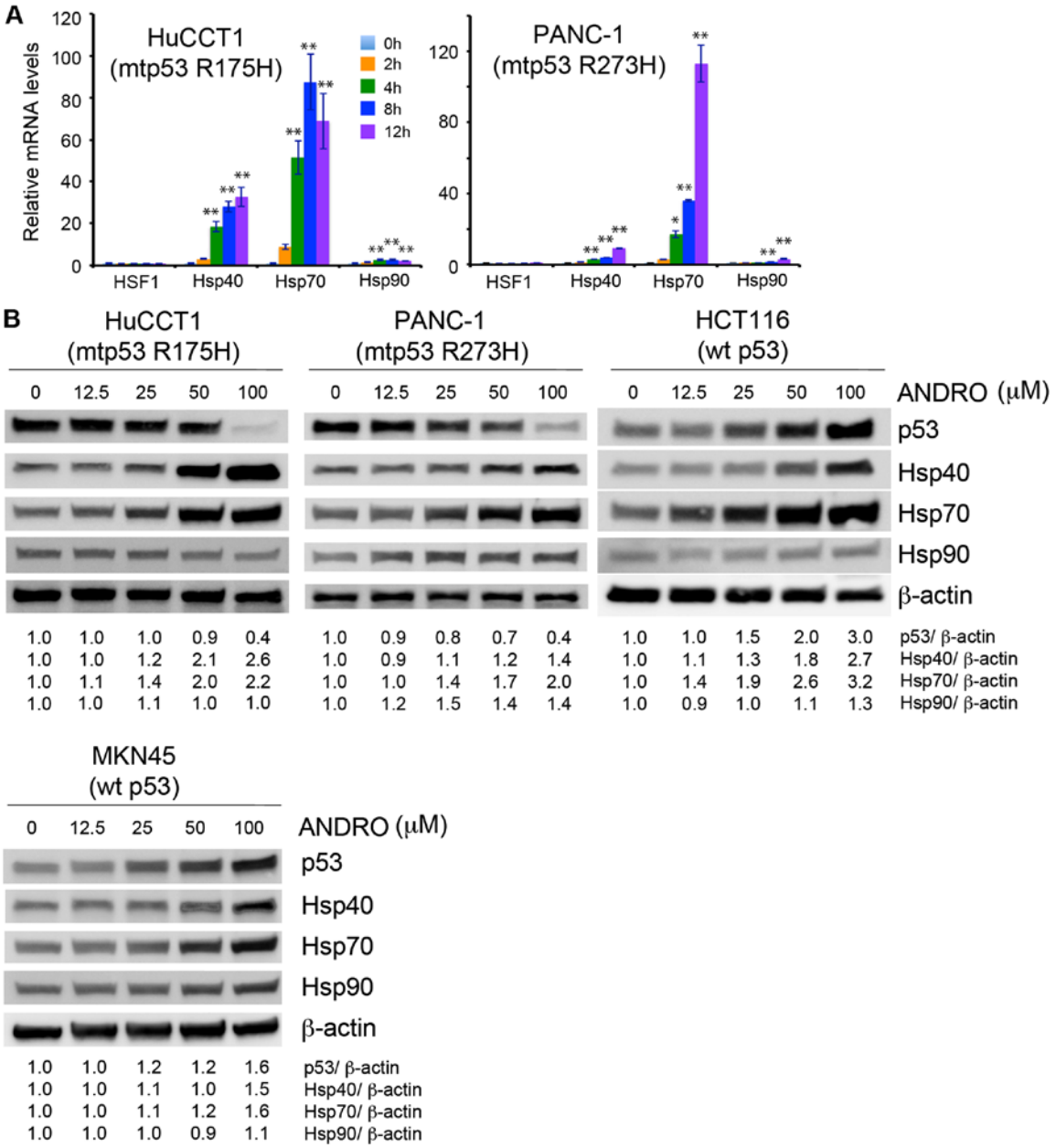

Figure 4. ANDRO induces mutant p53 degradation via Hsp70. (A) Reverse transcription-quantitative polymerase chain reaction analysis of HSF1, Hsp40, Hsp70, Hsp90 mRNA levels following treatment of cells expressing mutant p53 with ANDRO (100 μM). Values are presented as the mean ± standard deviation of three independent experiments performed in triplicate. *P<0.05, **P<0.01 vs. 0 h. (B) Heat-shock protein expression in cancer cells 18 h after treatment with ANDRO. Quantitative analysis was performed on each western blotting. mtp53, mutant p53; wt p53, wild-type p53; HSF1, heat shock transcription factor 1; Hsp, heat shock protein; ANDRO, andrographolide.

(10 mg/kg) administered via i.p. injection three times per week for 11 days. On day 12, the tumor volumes of HuCCT1 were: 352.8±86.8 mm^3 (range, 256-445.5 mm^3; maximum diameter, 10 mm) in the DMSO group; 130.3±11.5 mm^3 (range, 126-147.9 mm^3; maximum diameter, 7 mm) in the CPT-11 group; and 58.8±8.8 mm^3 (range, 45.6-75 mm^3; maximum diameter, 6 mm) in the ANDRO group (Fig. 7A), indicating that ANDRO was more effective than CPT-11 in suppressing the growth of mutant p53-expressing HuCCT1 cells *in vivo*. By contrast, CPT-11 was more effective than ANDRO at reducing the wild-type p53-expressing MKN45 tumor volumes: 425.7±124 mm^3 (range, 256-650 mm^3; maximum diameter, 11 mm) in the DMSO control group; 131.3±26.5 mm^3 (range, 108-171.5 mm^3; maximum diameter, 7 mm) in the CPT-11 group; and 195.6±87.1 mm^3 (range, 75-294 mm^3; maximum diameter, 10 mm) in the ANDRO group on day 12 (Fig. 7A). Notably, no significant body weight loss was observed in any of the mouse groups during the treatment period (Fig. 7B).

Discussion

Several small molecule anticancer drugs have been reported to target mutant p53. Some of these, such as PRIMA-1 (11), MIRA-1 (12), NSC319726 (13), stictic acid (14) and chetomin (15), function by reactivating mutant p53, thus re-establishing downstream target gene expression, and induction of cell cycle arrest and apoptosis. Another group of small molecules act by inhibiting mutant p53 gain-of-function

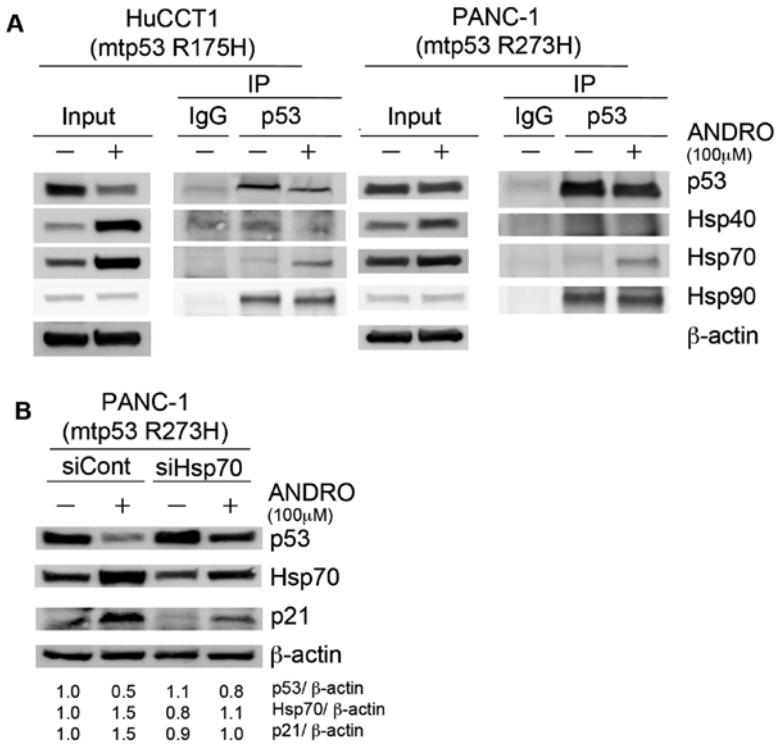

Figure 5. Hsp70 is responsible for degradation of mutant p53 under ANDRO treatment. (A) Co-immunoprecipitation experiments show increased Hsp70 binding to immunoprecipitated p53 upon ANDRO (100 μM) treatment of mutant p53-expressing HuCCT1 and PANC-1 cells for 18h. Input lysates and co-immunoprecipitated proteins were analyzed by immunoblotting with the indicated antibodies. (B) Knockdown of Hsp70 impairs the degradation of mutant p53. Cells were transfected with control or Hsp70-specific siRNAs and treated with ANDRO (100 μM) for 18 h. mtp53, mutant p53; IgG, immunoglobulin G; IP, immunoprecipitated; ANDRO, andrographolide; Hsp, heat shock protein; si, small interfering RNA; Cont, negative control.

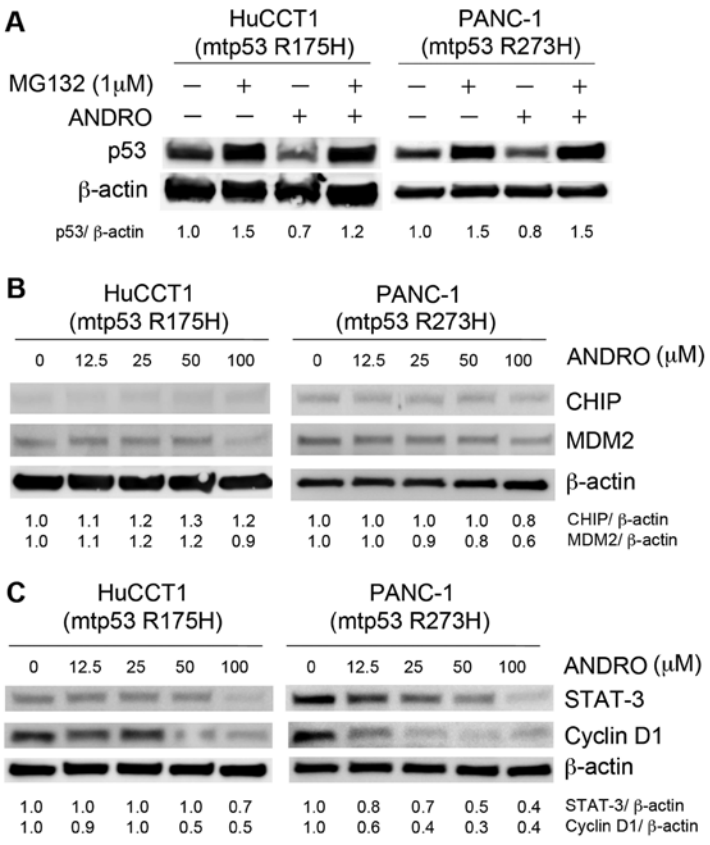

Figure 6. ANDRO induces proteasomal degradation of mtp53. (A) mtp53 protein levels in HuCCT1 and PANC-1 cells treated with MG132 (1 μM) and ANDRO (100 μM) for 18 h. Expression of (B) CHIP and MDM2, and (C) STAT-3 and cyclin D1 in mtp53 cancer cells after treatment with ANDRO for 18 h. Quantitative analysis was performed on each western blotting. mtp53, mutant p53; ANDRO, andrographolide; CHIP, E3 ubiquitin-protein ligase CHIP; MDM2, E3 ubiquitin-protein ligase Mdm2; STAT-3, signal transducer and activator of transcription 3.

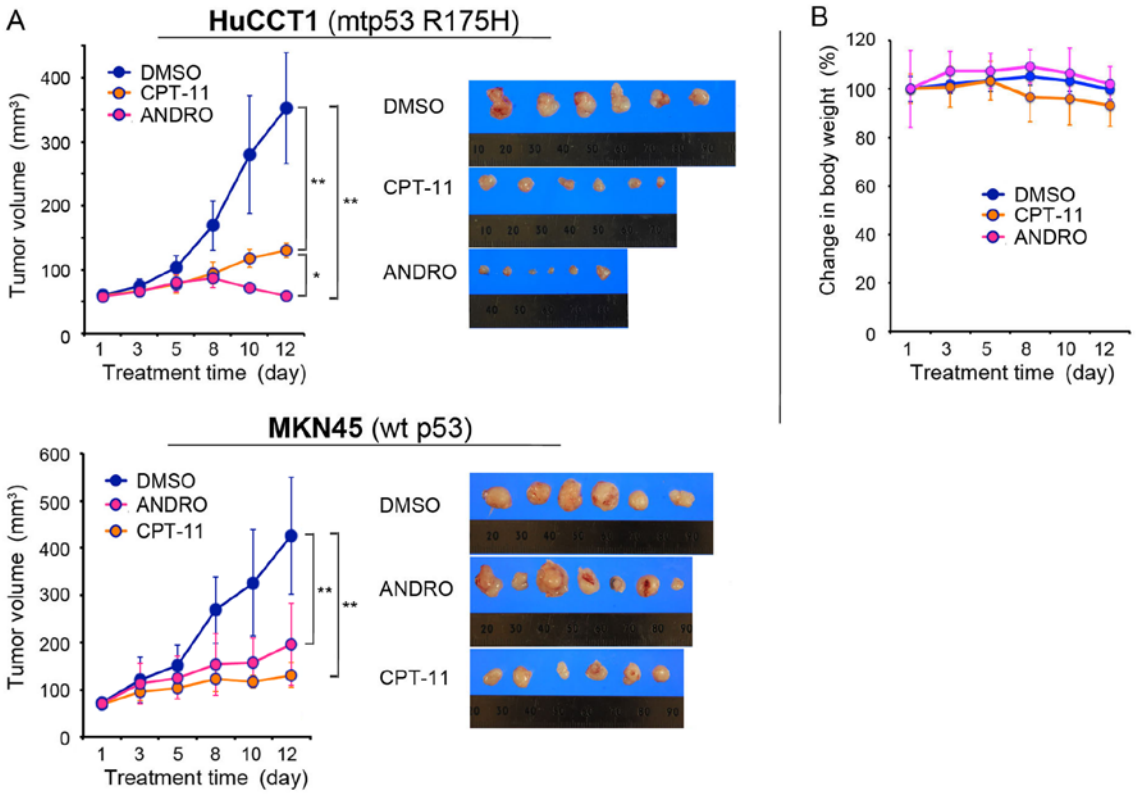

Figure 7. ANDRO suppresses tumor growth *in vivo*. HuCCT1 and MKN45 (n=6/group) tumor xenografts were allowed to grow to 50 mm^3 before the treatment. DMSO, ANDRO, or CPT-11 were injected intraperitoneally three times per week. (A) Tumor volumes. (B) Change in body weight of mouse. Values are presented as the mean ± standard deviation. *P<0.05, **P<0.01. mtp53, mutant p53; DMSO, dimethyl sulfoxide; wt p53, wild-type p53; CPT-1, irinotecan; ANDRO, andrographolide.

activities. These include histone deacetylase inhibitors (16,17), NSC59984 (18), gambogic acid (19), disulfiram (20), geldanamycin (21) and spautin-1 (22).

ANDRO was used in the current study as a small molecule inhibitor of mutant p53. ANDRO, a diterpenoid lactone, is a naturally occurring compound isolated from the stem and leaves of a traditional Chinese herb, *Andrographis paniculata*, and is commonly used to treat respiratory infections, fever and diarrhea (23). Traditional Chinese herbs are gaining increasing attention as a source of anticancer agents, particularly as they are easy to obtain and have few, if any, side effects (24). Previous studies have demonstrated that ANDRO possesses anti-inflammatory (25,26), anti-asthmatic (27), anti-viral (28) and hepatoprotective (29) activities, in addition to its various anticancer effects (30,31). However, the effect of ANDRO on mutant p53 has not previously been investigated.

In the current study, it was demonstrated that ANDRO induces the degradation of mutant p53 via increased Hsp70 expression. Several recent studies have also observed an association between heat-shock proteins and mutant p53 in cancer cells. Paradoxically, although Hsp70 contributes to the stability of mutant p53 (32), it may also be associated with the degradation of mutant p53 (33,34). In the present study, ANDRO increased the expression of Hsp70 and increased its binding to mutant p53. In addition, siRNA-mediated knockdown of Hsp70 impaired the ANDRO-mediated reduction in mutant p53 levels. These results indicated that increased Hsp70 activity is one mechanism by which ANDRO promotes the degradation of mutant p53 protein.

Two major pathways are thought to be responsible for decreasing mutant p53 protein levels; namely, proteasomal and autophagic degradation (22). The experiments with MG132 suggest that ANDRO acts via the proteasomal degradation pathway. Although MDM2 and CHIP, E3 ubiquitin ligases known to target p53, were not induced by ANDRO, we hypothesize that another E3 ubiquitin-related protein may mediate the degradation of mutant p53 in this study. This possibility would be clarified by mass spectrometric analysis of p53-interacting proteins.

The current study demonstrated that ANDRO has anticancer effects *in vitro* and *in vivo*. Although p21, PUMA, and NOXA are known to be induced by wild-type p53 protein, it was demonstrated here that they are also induced by ANDRO treatment of cells harboring mutant p53. One potential mechanism of the increased p21 levels may be independent of p53. Zhang *et al* (35) previously reported that MDM2 is a negative regulator of p21. The data of the current study revealed that MDM2 was marginally decreased following ANDRO treatment of mutant p53 cells. Another potential mechanism of p21 induction is via STAT-3 inactivation. Previous study has demonstrated that expression of p21 and apoptosis-associated proteins are regulated by STAT-3, and mutant p53 activates these proteins by suppressing the activity of STAT-3 and Akt (10). In the experiments of the present study, ANDRO inhibited STAT-3, suggesting a potential mechanism for its induction of p21 and apoptosis-associated proteins.

In the mouse xenograft model, ANDRO suppressed tumor growth irrespective of p53 mutational status, but the effect was

greater for mutant p53-expressing cells. As no significant body weight loss was observed in ANDRO-treated mice, ANDRO may be a potential treatment for mutant p53-expressing tumors, which constitute about half of all human cancers. In conclusion, the findings of the current study demonstrated that ANDRO induces the degradation of mutant p53 via activation of Hsp70.

Acknowledgements

Not applicable.

Funding

This study was partially supported by Grant-in Aid for the Young Scientists (B: 16K19938) from Japan Society for the Promotion of Science and Medical Care Education Research Foundation (Fukuoka, Japan).

Availability of data and materials

The data sets generated during the study are available from the corresponding author on reasonable request.

Authors' contributions

HS and MH conceived and designed the experiments. HS performed the majority of the experiments; TN and NE performed certain experiments. HS, TN and MH analyzed the data. HS and MH contributed to interpretation of the data, and were major contributors in writing the manuscript. TN, KB, TT and HN contributed to the research design and edited the manuscript. All authors read and approved the final manuscript.

Ethics approval and consent to participate

An animal experimental protocol was reviewed and approved by the Animal Care Committee of Saga University (Saga, Japan; permission no. 27-039-0).

Consent for publication

Not applicable.

Competing interests

The authors declare that they have no competing interests.

References

1. Joerger AC and Fersht AR: Structural biology of the tumor suppressor p53. Annu Rev Biochem 77: 557-582, 2008.
2. Lane DP: Cancer. p53, guardian of the genome. Nature 358: 15-16, 1992.
3. Hainaut P and Hollstein M: p53 and human cancer: The first ten thousand mutations. Adv Cancer Res 77: 81-137, 2000.
4. Terzian T, Suh YA, Iwakuma T, Post SM, Neumann M, Lang GA, Van Pelt CS and Lozano G: The inherent instability of mutant p53 is alleviated by Mdm2 or p16INK4a loss. Genes Dev 22: 1337-1344, 2008.
5. Bossi G, Lapi E, Strano S, Rinaldo C, Blandino G and Sacchi A: Mutant p53 gain of function: Reduction of tumor malignancy of human cancer cell lines through abrogation of mutant p53 expression. Oncogene 25: 304-309, 2006.
6. Patricia AM and Vousden KH: Mutant p53 in cancer. Cancer Cell 25: 304-317, 2013.
7. Livak KJ and Schmittgen TD: Analysis of relative gene expression data using real-time quantitative PCR and the 2(-Delta Delta C(T)) method. Methods 25: 402-408, 2001.
8. King FW, Wawrzynow A, Höhfeld J and Zylicz M: Co-chaperones Bag-1, Hop and Hsp40 regulate Hsc70 and Hsp90 interactions with wild-type or mutant p53. EMBO J 20: 6297-6305, 2001.
9. Li D, Marchenko ND, Schulz R, Fischer V, Velasco-Hernandez T, Talos F and Moll UM: Functional inactivation of endogenous MDM2 and CHIP by HSP90 causes aberrant stabilization of mutant p53 in human cancer cells. Mol Cancer Res 9: 577-588, 2011.
10. Bao GQ, Shen BY, Pan CP, Zhang YJ, Shi MM and Peng CH: Andrographolide causes apoptosis via inactivation of STAT3 and Akt and potentiates antitumor activity of gemcitabine in pancreatic cancer. Toxicol Lett 222: 23-35, 2013.
11. Lambert JM, Gorzov P, Veprintsev DB, Söderqvist M, Segerbäck D, Bergman J, Fersht AR, Hainaut P, Wiman KG and Bykov VJ: PRIMA-1 reactivates mutant p53 by covalent binding to the core domain. Cancer Cell 15: 376-388, 2009.
12. Bykov VJ, Issaeva N, Zache N, Shilov A, Hultcrantz M, Bergman J, Selivanova G and Wiman KG: Reactivation of mutant p53 and induction of apoptosis in human tumor cells by maleimide analogs. J Biol Chem 280: 30384-30391, 2005.
13. Yu X, Vazquez A, Levine AJ and Carpizo DR: Allele-specific p53 mutant reactivation. Cancer Cell 21: 614-625, 2012.
14. Wassman CD, Baronio R, Demir Ö, Wallentine BD, Chen CK, Hall LV, Salehi F, Lin DW, Chung BP, Hatfield GW, *et al*: Computational identification of a transiently open L1/S3 pocket for reactivation of mutant p53. Nat Commun 4: 1407, 2013.
15. Hiraki M, Hwang SY, Cao S, Ramadhar TR, Byun S, Yoon KW, Lee JH, Chu K, Gurkar AU, Kolev V, *et al*: Small-molecule reactivation of mutant p53 to wild-type-like p53 through the p53-Hsp40 regulatory axis. Chem Biol 22: 1206-1216, 2015.
16. Li D, Marchenko ND and Moll UM: SAHA shows preferential cytotoxicity in mutant p53 cancer cells by destabilizing mutant p53 through inhibition of the HDAC6-Hsp90 chaperone axis. Cell Death Differ 18: 1904-1913, 2011.
17. Blagosklonny MV, Trostel S, Kayastha G, Demidenko ZN, Vassilev LT, Romanova LY, Bates S and Fojo T: Depletion of mutant p53 and cytotoxicity of histone deacetylase inhibitors. Cancer Res 65: 7386-7392, 2005.
18. Zhang S, Zhou L, Hong B, van den Heuvel AP, Prabhu VV, Warfel NA, Kline CL, Dicker DT, Kopelovich L and El-Deiry WS: Small-molecule NSC59984 restores p53 pathway signaling and antitumor effects against colorectal cancer via p73 activation and degradation of mutant p53. Cancer Res 75: 3842-3852, 2015.
19. Wang J, Zhao Q, Qi Q, Gu H, Rong J, Mu R, Zou M, Tao L, You Q and Guo Q: Gambogic acid-induced degradation of mutant p53 is mediated by proteasome and related to CHIP. J Cell Biochem 112: 509-519, 2011.
20. Paranjpe A, Srivenugopal KS: Degradation of NF-kappaB, p53 and other regulatory redox-sensitive proteins by thiol-conjugating and -nitrosylating drugs in human tumor cells. Carcinogenesis 34: 990-1000, 2013.
21. Lin K, Rockliffe N, Johnson GG, Sherrington PD and Pettitt AR: Hsp90 inhibition has opposing effects on wild-type and mutant p53 and induces p21 expression and cytotoxicity irrespective of p53/ATM status in chronic lymphocytic leukaemia cells. Oncogene 27: 2445-2455, 2008.
22. Liu J, Xia H, Kim M, Xu L, Li Y, Zhang L, Cai Y, Norberg HV, Zhang T, Furuya T, *et al*: Beclin1 controls the levels of p53 by regulating the deubiquitination activity of USP10 and USP13. Cell 147: 223-234, 2011.
23. Akbar S: *Andrographis paniculata*: A review of pharmacological activities and clinical effects. Altern Med Rev 16: 66-77, 2011.
24. Xia Q and Mao W: Anti-tumor effects of traditional Chinese medicine give a promising perspective. J Cancer Res Ther 10 (Suppl 1): 1-2, 2014.
25. Abu-Ghefreh AA, Canatan H and Ezeamuzie CI: In vitro and in vivo anti-inflammatory effects of andrographolide. Int Immunopharmacol 9: 313-318, 2009.
26. Shao ZJ, Zheng XW, Feng T, Huang J, Chen J, Wu YY, Zhou LM, Tu WW and Li H: Andrographolide exerted its antimicrobial effects by upregulation of human β-defensin-2 induced through p38 MAPK and NF-κB pathway in human lung epithelial cells. Can J Physiol Pharmacol 90: 647-653, 2012.

27. Nguyen VS, Loh XY, Wijaya H, Wang J, Lin Q, Lam Y, Wong WS and Mok YK: Specificity and inhibitory mechanism of andrographolide and its analogues as antiasthma agents on NF-κB p50. J Nat Prod 78: 208-217, 2015.
28. Wintachai P, Kaur P, Lee RC, Ramphan S, Kuadkitkan A, Wikan N, Ubol S, Roytrakul S, Chu JJ and Smith DR: Activity of andrographolide against chikungunya virus infection. Sci Rep 5: 14179, 2015.
29. Thingale AD, Shaikh KS, Channekar PR, Galgatte UC, Chaudhari PD and Bothiraja C: Enhanced hepatoprotective activity of andrographolide complexed with a biomaterial. Drug Deliv 22: 117-124, 2015.
30. Zhang QQ, Ding Y, Lei Y, Qi CL, He XD, Lan T, Li JC, Gong P, Yang X, Geng JG, *et al*: Andrographolide suppress tumor growth by inhibiting TLR4/NF-κB signaling activation in insulinoma. Int J Biol Sci 10: 404-414, 2014.
31. Gao H and Wang J: Andrographolide inhibits multiple myeloma cells by inhibiting the TLR4/NF-κB signaling pathway. Mol Med Rep 13: 1827-1832, 2016.
32. Wiech M, Olszewski MB, Tracz-Gaszewska Z, Wawrzynow B, Zylicz M and Zylicz A: Molecular mechanism of mutant p53 stabilization: The role of HSP70 and MDM2. PLoS One 7: e51426, 2012.
33. Kim HB, Lee SH, Um JH, Oh WK, Kim DW, Kang CD and Kim SH: Sensitization of multidrug-resistant human cancer cells to Hsp90 inhibitors by down-regulation of SIRT1. Oncotarget 6: 36202-36218, 2015.
34. Buckley NE, D'Costa Z, Kaminska M and Mullan PB: S100A2 is a BRCA1/p63 coregulated tumour suppressor gene with roles in the regulation of mutant p53 stability. Cell Death Dis 5: e1070, 2014.
35. Zhang Z, Wang H, Li M, Agrawal S, Chen X and Zhang R: MDM2 is a negative regulator of p21WAF1/CIP1, independent of p53. J Biol Chem 279: 16000-16006, 2004.